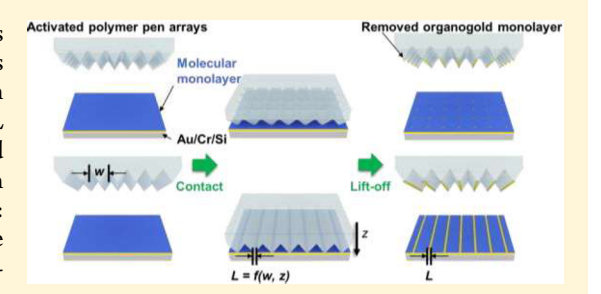


Polymer-Pen Chemical Lift-Off Lithography

Xiaobin Xu, †,\ddagger_0 Qing Yang, †,\ddagger_0 Kevin M. Cheung, †,‡ Chuanzhen Zhao, †,\ddagger_0 Natcha Wattanatorn, †,‡ Jason N. Belling, †,‡ John M. Abendroth, †,‡ Liane S. Slaughter, †,‡ Chad A. Mirkin, $^{\perp,\#_0}$ Anne M. Andrews, $^{*,\dagger,\ddagger,\sharp_0}$ and Paul S. Weiss $^{*,\dagger,\ddagger,\$_0}$

Supporting Information

ABSTRACT: We designed and fabricated large arrays of polymer pens having sub-20 nm tips to perform chemical lift-off lithography (CLL). As such, we developed a hybrid patterning strategy called polymer-pen chemical lift-off lithography (PPCLL). We demonstrated PPCLL patterning using pyramidal and v-shaped polymer-pen arrays. Associated simulations revealed a nanometer-scale quadratic relationship between contact line widths of the polymer pens and two other variables: polymer-pen base line widths and vertical compression distances. We devised a stamp support system consisting of interspersed arrays of flattipped polymer pens that are taller than all other sharp-tipped polymer



pens. These supports partially or fully offset stamp weights thereby also serving as a leveling system. We investigated a series of vshaped polymer pens with known height differences to control relative vertical positions of each polymer pen precisely at the sub-20 nm scale mimicking a high-precision scanning stage. In doing so, we obtained linear-array patterns of alkanethiols with sub-50 nm to sub-500 nm line widths and minimum sub-20 nm line width tunable increments. The CLL pattern line widths were in agreement with those predicted by simulations. Our results suggest that through informed design of a stamp support system and tuning of polymer-pen base widths, throughput can be increased by eliminating the need for a scanning stage system in PPCLL without sacrificing precision. To demonstrate functional microarrays patterned by PPCLL, we inserted probe DNA into PPCLL patterns and observed hybridization by complementary target sequences.

KEYWORDS: Chemical patterning, soft lithography, microcontact printing, nanolithography, alkanethiols, DNA hybridization

C ubstantial progress has been made in chemical patterning methods to push resolution from micron to nanometer scales for applications in electronics, 1-7 optics, 8,9 energy, 10,11 and biology, ^{12,13} for example, integrated circuits, ^{14–16} displays, ^{17–19} ultrasensitive biosensors, ^{20–25} nanomotors, ²⁶ biomolecule micro/nano-arrays, ^{27–31} wearable sensors, ^{32–35} and other advanced metamaterials.³⁶ Nano- and microfabrication are dominated by patterning methods based on energetic beams, such as light, electrons, ions, and X-rays. Conventional photolithography can be used to fabricate structures over large areas, however, resolution is limited and costs of the masks are high. Advanced lithography techniques, such as liquid immersion/multiple patterning photolithography, 37,38 X-ray lithography, ^{39,40} or extreme ultraviolet photolithography, ^{41–43} can push resolution to nanometer scales but availability is limited due to high setup and maintenance costs. Direct-write techniques, such as electron-beam lithography (EBL)⁴⁴⁻⁵⁰ and focused ion-beam lithography (FIB)^{51,52} are used to generate nanoscale patterns but time-consuming serial writing processes limit their throughput.⁵³

Without using energetic beams, microcontact printing (μ CP) is a high-throughput, straightforward molecular printing technique for chemical patterning at the micro- and nanometer scales. 54,55 Microcontact printing involves elastomeric stamps with molecular "inks" such as organic molecules, proteins, or DNA that enables ink transfer to planar or curved substrates composed of metals, glass, or polymers to produce patterns. Organic ink molecules, such as alkanethiols, serve as molecular resists in successive wet etching steps to transfer patterns to underlying substrates, for example, metals. 56,57 Nonetheless, ink molecules are known to diffuse laterally beyond the contact areas during printing, resulting in resolution limited to ~100 nm for μCP . 58-60

We have developed strategies to minimize or to eliminate lateral diffusion of ink molecules via modified μ CP methods. 61–66 For example, microdisplacement printing 67,68 and microcontact insertion printing 59,69 are used to print

Received: March 23, 2017 Revised: April 12, 2017 Published: April 14, 2017

[†]California NanoSystems Institute, [‡]Department of Chemistry and Biochemistry, [§]Department of Materials Science and Engineering, and Department of Psychiatry and Biobehavioral Health, Semel Institute for Neuroscience and Human Behavior, and Hatos Center for Neuropharmacology, University of California, Los Angeles, Los Angeles, California 90095, United States

¹Department of Chemistry and International Institute for Nanotechnology and [#]Department of Materials Science and Engineering, Northwestern University, Evanston, Illinois 60208, United States

molecules on alkanethiol self-assembled monolayer (SAM)modified substrates through displacement or insertion processes, respectively. The SAMs in the unpatterned regions prevent ink molecules from diffusing beyond the contact areas. 59,70 We also developed a "subtractive" stamping process called chemical lift-off lithography (CLL), 60,71 in which oxygen plasma-activated polydimethylsiloxane (PDMS) stamps selectively remove hydroxyl- (-OH) (or other sufficiently reactive groups such as amine-) terminated alkanethiols only in the contact areas with high pattern fidelity and without observable lateral diffusion. The remaining SAM molecules in the nonlifted-off regions act as resists for selective etching of exposed gold in the patterned regions. High-fidelity chemical patterns with line widths as narrow as 40 ± 2 nm were achieved using CLL with features reaching 20 nm via double patterning⁶⁰ and even 5 nm (corresponding to patterns about 10 molecules across).⁷¹ However, for CLL, like μ CP, the fabrication of masters with nanometer-scale resolution relies on lowthroughput, high-cost EBL/FIB limiting applicability.

Dip-pen lithography can write chemical patterns directly on substrates at sub-50 nm resolution by using atomic force microscopy with tip-coated molecular "inks", for example, alkanethiols, but again, throughput is low due to timeconsuming serial writing. 72 Polymer-pen lithography $(PPL)^{73-78}$ combines high-resolution dip-pen lithography and μ CP by using a scanning stage equipped with massively parallel polymer-pen arrays (with sub-80 nm tip diameters) to write patterns with ink molecules directly at ~100 nm resolution with high throughput.⁷³ Reusable masters for producing polymer pens are fabricated by conventional photolithography at micron-scale resolution via anisotropic etching of Si(100).⁷³ The use of a scanning stage enables nanometer-scale control of polymer pens in the x, y, and zplanes. Another advantage of PPL is that feature sizes can be tuned from 80 nm to >10 μ m by varying dwell times and vertical pen compression in a single stamp. ⁷⁶ However, lateral diffusion of ink molecules persists limiting the resolution of PPL similar to issues with μ CP.

To advance feature resolution in chemical patterning in highly multiplexed and facile directions, we developed a hybrid method termed polymer-pen chemical lift-off lithography (PPCLL) that combines the advantages of PPL (massively parallel polymer pens with nanometer-scale tips for highthroughput patterning and feature size tunability by controlling vertical compression distances) and CLL (high-fidelity patterning without lateral diffusion) to enable large-area, lowcost, and sub-20 nm resolution patterning capabilities simultaneously. Fabrication of polymer pens with nanometersized tip diameters is described (Scheme S1). Films of 500 nmthick SiO₂ were grown on 4 in. Si(100) wafers via thermal oxidation, followed by spin coating with photoresist (SPR700-1.2). Conventional photolithography was then used to create micron-scale square or line array patterns on photoresist-coated SiO₂/Si(100) wafers. The line widths of the masters govern the base line widths of the polymer pens. Overall areas are 1.5 cm \times 1.5 cm for each square or line array pattern. It is critical to align edge axes of the square/line features on each photomask such that they are parallel with the primary flat edge of each Si(100) wafer, which is parallel to the (110) direction of Si(100). Imperfect alignment resulted in blunt pen tips.

Next, reactive ion-etching (RIE) was used to etch exposed SiO_2 selectively to reveal the underlying Si(100). Subsequently, a solution with a 4:1 ratio of 30% KOH and isopropanol was

used to etch Si(100) wafers anisotropically to generate arrays of recessed pyramidal structures (from patterns of squares) or v-shaped structures (from patterns of lines) having base dimensions matched to the designed patterns in the photomasks. The Si master fabrication was completed by removing remaining SiO₂ in 25% HF solution for 5 min. Finally, PDMS stamps containing arrays of polymer pens were produced from the masters. Both the masters and stamps can be reused many times. (Experimental details are provided in the Supporting Information.)

As shown in the scanning electron microscopy (SEM) images in Figure 1, high-quality Si masters containing large

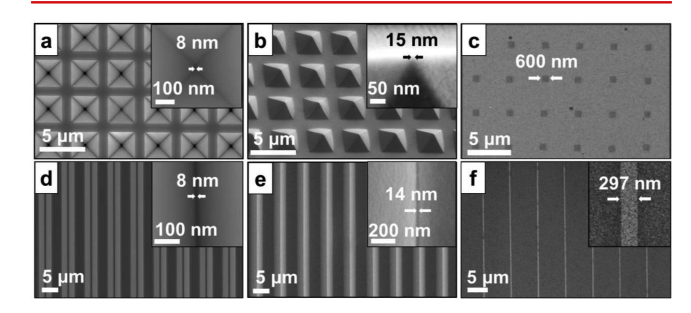


Figure 1. Scanning electron microscopy (SEM) images of (a) Si master with recessed pyramidal structures having base line widths of 3 μ m and a periodicity of 4 μ m; (b) polydimethylsiloxane (PDMS) stamp with pyramidal polymer-pen arrays replicated from the master in (a); (c) polymer-pen chemical lift-off lithography (PPCLL) pattern produced using the stamp in (b) without external compression; (d) Si master with recessed v-shaped structures with base line widths of 3.8 μ m and a periodicity of 7 μ m; (e) PDMS stamp with v-shaped polymer pen arrays replicated from the master in (d); (f) typical PPCLL pattern produced using the stamp in (b) without external compression. (Insets: high-magnification SEM images.) (The images (c,f) are processed to visualize the patterns better; the unprocessed images are shown in Figures S3.)

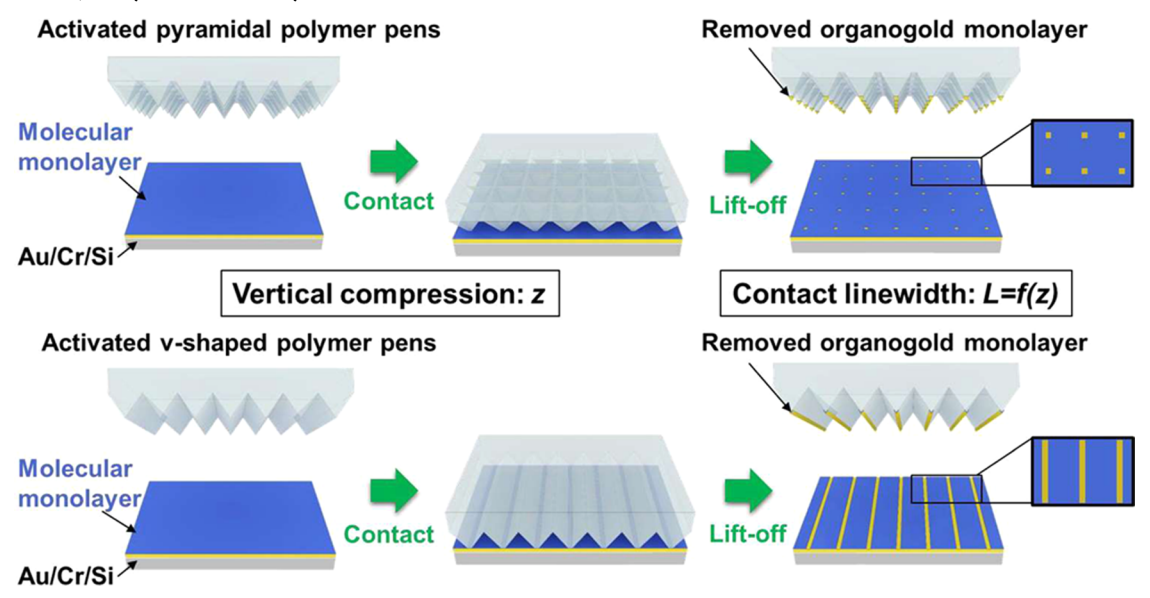
arrays of recessed pyramidal or v-shaped structures and stamps containing large arrays of protruding pyramidal/v-shaped polymer pens were fabricated using this method. The recessed pyramids or v-shaped structures of the masters had typical tip diameters $d_{\rm tip}$ of 8 nm, whereas protruding pyramids and v-shaped polymer pens had average measured tip diameters $d_{\rm tip}$ of 19 \pm 2 and 15 \pm 2 nm, respectively. Typical polymer pen tips with $d_{\rm tip}$ of 15 and 14 nm are shown in the insets of Figure 1.

The larger tip diameters of the features on the PDMS stamps compared to those of the masters were likely due to a tiprounding effect caused by the high surface tension of PDMS when it is applied to the masters (and before curing). The sub-20 nm tip-diameters $d_{\rm tip}$ of the polymer pens are comparable to the smallest features fabricated using EBL, however, polymer pens produced by the method described above avoid EBL and thus, the need to produce each set of pens serially. Average tip diameters of the polymer pens fabricated here are smaller than most reported polymer pens (usually >50 nm), because the square or narrow rectangular features on the photomasks have small widths (<6 μ m) and their edges were perfectly aligned to Si (110) directions to allow Si{111} facets to converge into sharp points or sharp lines during the anisotropic etching of Si(100).

As-fabricated PDMS stamps with polymer pen arrays were used in PPCLL as illustrated in Scheme 1.

Step 1: A 40 s O₂ plasma treatment generated hydrophilic siloxy (Si—OH) groups on PDMS stamp surfaces containing

Scheme 1. Schematic Illustrations of Polymer-Pen Chemical Lift-off Lithography (PPCLL) Using Pyramidal (Top) and V-Shaped (Bottom) Polymer Pen Arrays^a



"In both cases, in the first step hydroxyl-terminated alkanethiol molecules form self-assembled monolayers (SAMs) on Au/Cr/Si substrates. The polydimethylsiloxane (PDMS) stamps carrying the polymer-pen arrays are then activated with oxygen plasma treatment. In the second step, an activated PDMS stamp is brought into conformal contact with the SAM on a Au/Cr/Si substrate using a known vertical compression distance. Condensation reactions occur between the hydroxyl-terminated SAM molecules and the activated PDMS stamp to form strong covalent bonds. In the third step, the PDMS stamp is lifted off of the substrate, removing a portion of SAM molecules (\sim 70%) together with Au adatoms from the contact areas to produce a complementary pattern on the substrate and an organogold monolayer on the stamp in the regions of contact. The contact/feature line width (L) is controlled by the vertical compression distance (z) of the stamp during contact via the relationship L = f(z).

pyramidal/v-shaped polymer pens. This step is called "activation".⁸¹

Step 2: Activated PDMS stamps were brought into conformal contact with Au/Cr/Si substrates (Au, 100 nm over Cr, 5 nm) functionalized with hydroxyl-terminated alkanethiol SAM molecules by gently placing each stamp on a substrate by hand. 11-Mercapto-1-undecanol SAM molecules were used throughout this study, but alkanethiols with other backbones, chain lengths, and terminal functional groups can be used. A condensation reaction occurs between Si—OH groups on activated PDMS stamps and the terminal hydroxyl groups of the self-assembled alkanethiol molecules to form covalent bonds, that is, Si—O—SAM thereby enabling lift-off.

Step 3: The PDMS stamps were removed to lift-off SAM molecules only in the contact areas producing complementary patterns of SAMs on the Au/Cr/Si substrates. Note that in this lift-off process, a layer of Au adatoms is removed along with the lifted SAM molecules. We hypothesize that this occurs because weaker Au—Au bonds in the top layer of the substrate surfaces are preferentially broken during lift-off, rather than the Au—S bonds between the substrate and alkanethiols.⁶⁰

As previously reported, ^{76,77} deformation of polymer pens and thus the areas contacted by each pen can be controlled in PPL by compressing the polymer pens onto the substrates using a scanning stage with vertical compression-distance control. For example, square features can be obtained with line widths ranging from 500 to 2000 nm by controlled vertical compression with submicron increments. ⁷⁶ However, time-dependent lateral diffusion results in larger feature sizes than actual contact areas in PPL. By contrast, in PPCLL, patterned features and contact areas are *identical* in size. If the vertical compression distance is controlled at the nanometer-scale, then presumably contact areas can be correspondingly controlled.

However, in practice nanometer-scale differences in deformation and contact areas are challenging.

Alternately, computational simulations can be used to predict deformation at the nanometer scale. Here, we simulated compression of v-shaped polymer pens in addition to the more well-studied pyramidal polymer pens. 76,82 Zheng et al. simulated deformation of pyramidal polymer pens and found that contact radii increased linearly with vertical compression distances from sub-100 nm to submicron with nanometer-scale resolution.⁸² To simulate the vertical compression-distancedependent deformation of v-shaped polymer pens at the nanometer scale, we constructed a 2D Mooney-Rivlin model using a finite-element method via ANSYS software (Ansys Inc., Canonsburg, PA). We simulated vertical compression distances (z) from 0 to 560 nm with a minimum step size in z of 2 nm for v-shaped polymer pens having a base line width (w) = 4000nm and a tip diameter of 22 nm. An element size of 8 nm was used to model polymer-pen tips (from the tip to 400 nm in height). For the remainder of the polymer-pen height, an element size of 40 nm was used.

The initial contact was set to occur at a vertical compression distance of z = 10 nm. As shown in Figure 2, as z increased, the v-shaped polymer pen tips flattened and the contact line widths (L) increased. After fitting, we found a quadratic dependence between z and L at w = 4000 nm

$$L = f(z) = a + bz + cz^2 \tag{1}$$

where a=0 nm, b=0.444, $c=5.72\times 10^{-4}$ nm⁻¹, z>10 nm with L in nanometers. According to eq 1, we can precisely and robustly control the feature size by controlling z. Note that the standard deviation of the difference between the simulation results and fitted curve is only 1.4 nm and can be further reduced by decreasing the element size and step size in the

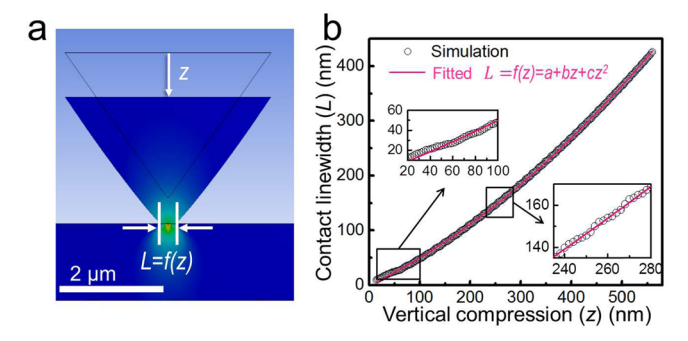


Figure 2. (a) Simulation: cross-sectional view of a v-shaped polymer pen (base line width, $4 \mu m$) vertically compressed onto a rigid Au surface with a vertical compression distance of z and a resulting contact line width of L = f(z). (b) Simulation results: increasing the vertical compression distance z leads to increased contact line width (L). The relationship between vertical compression distance z and L is fitted using the quadratic equation $L = f(z) = a + bz + cz^2$, where a, b, and c are constants.

simulations. Therefore, eq 1 accurately represents the relationship between z and L.

The above simulations demonstrate that feature-size resolution can be tuned at the nanometer scale in PPCLL. However, in practical experiments resolution is affected by the following additional factors: (a) precision of vertical compression distance, which relies solely on the resolution of the scanning stage, typically, a piezoelectric stage has a resolution <1 nm; and (b) surface smoothness of the polymer pens and substrates. As shown in Figure S1, atomic force microscopy characterization shows that the surfaces used here have an arithmetic average roughness (R_a) of 0.4 ± 0.1 nm for a recessed structure in the master and 1.1 ± 0.1 nm for a polymer pen. The value of R_a for the Au/Cr/Si substrate is ~ 1 nm (data not shown).

The integration of a piezoelectric scanning stage^{75,77} and a high-quality leveling technique into PPCLL, such as an optical-

or force-feedback leveling system, would enable an ultimate theoretical resolution of <2 nm to be reached. Without using these advanced equipment-intensive techniques, we nevertheless demonstrate nanometer-scale feature size control in PPCLL by designing and implementing a stamp support system and polymer pen arrays with height gradients, as described in the following experiments and simulations.

In the first experiment, activated PDMS stamps containing large arrays (3750 \times 3750 and 1 \times 2150) of pyramidal (w=3 μm , period = 4 μm) or v-shaped polymer pens (w=3.8 μm , period = 7 μm) were placed on substrates without external compression. Stamps conformally contacted substrates without the need for a leveling system. The contact time was set to 4–6 h to ensure high-quality pattern transfer. Our previous CLL work showed features could be transferred with contact times as short as 1 min; however, shorter contact times resulted in poorer features after wet etching.

The PPCLL patterns were imaged by SEM. The different intensities observed in SEM images were due to different chemical components on the surfaces.⁵⁹ As shown in Figure 1c,f, a square-dot array pattern (~600 nm line width) and a line-array pattern (~300 nm line width) were achieved. Moreover, the lateral diffusion of ink molecules was avoided in PPCLL, otherwise much enlarged features would have been observed after such long contact times. 59,76 The periodicities of the dot/line arrays were consistent with the stamp patterns. The enlarged feature sizes, compared to the original 20 nm tip diameters, were the result of polymer pen deformation caused by the weight of the stamps, which increased the contact line width to >20 nm. However, features were still 1-2 orders of magnitude smaller than the base line widths of the polymer pens in the photomask. Without using sophisticated fabrication techniques, we achieved submicron feature scales over large areas simply by this "contact and lift" process. Although there are nonuniform stress distributions in the contact region between each polymer pen and the substrate (e.g., in Figure 2a, the contact center has larger stress than the surrounding

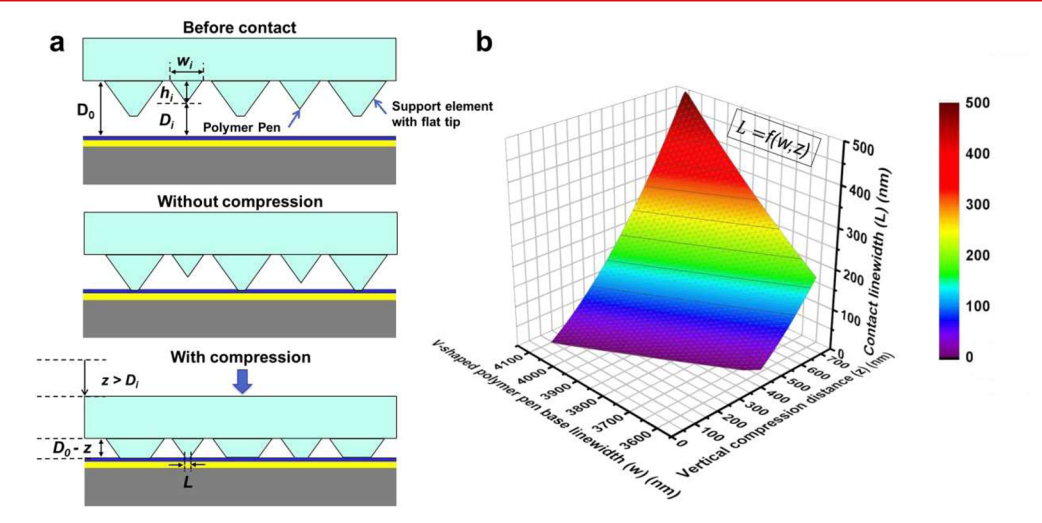


Figure 3. (a) Illustration of a polydimethylsiloxane (PDMS) stamp used in polymer-pen chemical lift-off lithography (PPCLL) having support elements (taller v-shaped polymer pens with flat tips) interleaved with v-shaped polymer pens (sharp tips with designed base line widths w_i): before contact, after placement on a substrate but with no vertical compression, and after vertical compression. Here, D_0 ($D_0 > h_i$) is the initial vertical distance from the base of the polymer pens to the surface of each substrate before contact; h_i is the height of a polymer pen; D_i is distance from the polymer pen tip to the substrate, $D_i = D_0 - h_i$; z is the vertical compression distance and L is resulting contact line width. (b) Simulation of results where v-shaped polymer pen base line widths (w) and vertical compression distances (z) were varied to control contact-dependent line widths (L), that is, L = f(w, z).

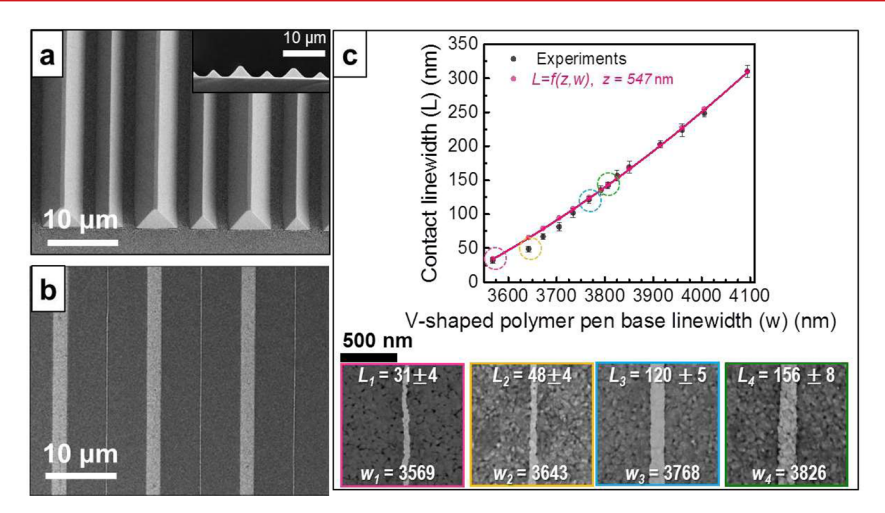


Figure 4. (a) A scanning electron microscopy (SEM) image of a polymer-pen array having designed height gradients and a stamp support system. Inset: cross-sectional view to show height differences. (b) An SEM image of a polymer-pen chemical lift-off lithography (PPCLL) pattern produced by the stamp in (a). (c) A plot of experimental and simulation results of the relationship between the line widths of the PPCLL patterns and the v-shaped polymer pen base line widths. Below are four SEM images of typical PPCLL patterned lines corresponding to the four data points circled in different colors. Note, L_1 , L_2 , L_3 , and L_4 are measured line widths; w_1 , w_2 , w_3 , and w_4 are the corresponding base line widths in nanometers. (The images (b) and insets of (c) are processed to visualize the patterns better; the unprocessed images are shown in Figures S3 and S4.).

region), the contact area remains the determining factor for the feature sizes. In addition, any small disruptions during the stamp placement and removal processes appear to have little influence on the features. In all PPCLL experiments so far, we successfully obtained the targeted chemical patterns without noticeable defects. Our results demonstrate that PPCLL is an economical, robust, and high-throughput method for producing submicron features over large areas.

We learned from the first set of experiments that the stamp weight deforms the tips such that no leveling is necessary. The height of each pyramidal/v-shaped polymer pen (h) is determined by its base line width (w) using the equation: $h = \frac{w}{2} \cdot \tan \theta = \frac{w}{\sqrt{2}}$, here θ is the angle between the Si(100) and Si(111) facets. Thus, polymer pens with a series of different base line widths (w_i) have different heights (h_i) by design. As illustrated in Figure 3a, the distances $(D_i = D_0 - h_i)$ from the tip of each polymer pen to the surface are different, where the subscript i (i > 0) is used to distinguish different polymer pens, and D_0 ($D_0 > h_i$) is the initial vertical distance from the base of the polymer pens to the surface of each substrate before contact. Under conformal contact, all of the polymer pens have the same initial vertical compression distance, z. However, upon initial contact with the substrate and due to their height differences, each polymer pen has a different effective vertical compression distance, $z_i' = z - D_i$. Contact only occurs when $z_i' > 0$, that is, $z > D_i$. Each contacted polymer pen has a contact line width, $L = f(z_i)$. We hypothesize that this process would be similar to vertical compression distances in PPCLL controlled using a piezoelectric scanning stage system.

To test this hypothesis, we added the base line width w as another variable in our simulations in addition to the vertical compression distance z, that is, L = f(w, z). In this simulation, we designed arrays with a series of w values ranging from 3500 to 4000 nm in increments of 25 nm. The initial vertical distance from the base of all of the v-shaped polymer pens to the surfaces of substrates was set at $D_0 = 3000$ nm, which is a reasonable distance to keep all of the v-shaped polymer pens from contacting the substrates. Then, vertical compression distances z, ranging from 0 to 700 nm with a step size of 5 nm,

were applied in the contact simulation between each v-shaped polymer pen and the substrate. After fitting the simulation results for all of the polymer pens with L = f(z), we derived a series of fitted curves. We plotted and connected all the fitted curves in the same three-dimensional space to form a curved surface. The curved surface was well fit by

$$L = f(z, w) = a + bz + cw + dzw + ez^{2} + fw^{2}$$
 (2)

where a = 2783, b = -2.786, c = -1.602, $d = 7.572 \times 10^{-4}$, $e = 5.729 \times 10^{-4}$, and $f = 2.232 \times 10^{-4}$ (the fitted curved surface is plotted in Figure 3b). The eq 2 is a universal equation wherein we can design and control desired contact line widths L either through w or z. Furthermore, when z is fixed w becomes the only variable influencing L. Under these conditions, eq 2 is reduced to

$$L = f(w) = a'' + b''w + c''w^{2}$$
(3)

On the basis of the above simulation results, in the second experiment we added two components in PPCLL, that is, a stamp support system and polymer pens with height gradients. The supporting elements are taller polymer pens with flat tips (obtained by incomplete anisotropic etching of Si(100)) distributed between the polymer pens used for pattering, as illustrated in Figure 3a. Here, the support elements have fixed base line widths of 6 μ m (Figure 4a). These support elements serve as weight-bearing pillars to support the stamp⁵⁶ and the flat tips further serve as a low-cost leveling system. Properly designed support elements can either keep the patterningpurpose polymer-pen arrays away from the substrate by fully canceling the weight of the stamp or they can control the degree of tip deformation of the patterning-purpose polymer pens by partially offsetting the stamp weights. The support elements can also be integrated into other PPL designs as an initial contact indicator to estimate how much extra vertical compression distance or force is needed to obtain desired contact areas.^{75,7}

For the second component, a series of v-shaped polymer pen arrays was designed with base line widths from 3500 to 4000 nm, as listed in Table 1. The support elements were designed

Table 1. Measured and Simulated Patterning Results of Polymer-Pen Chemical Lift-off Lithography Using Stamp Support
Elements and v-Shaped Polymer Pens over a Series of Designed Base Line Widths ^{a,b}

$w_{ m design}$	$w_{ m measured}$	$L_{ m measured}$	$L_{ m simulated}$	$\Delta w_{ m design}$	$\Delta w_{ m measured}$	$\Delta h_{ m calculated}$	$\Delta L_{ m measured}$
3500	3569	31 ± 4	34				
3550	3643	48 ± 4	65	50	74	52	17
3575	3673	67 ± 4	79	25	30	21	18
3600	3706	81 ± 7	94	25	33	23	14
3625	3735	101 ± 7	108	25	29	21	20
3650	3768	120 ± 5	124	25	33	23	19
3675	3792	134 ± 7	136	25	24	17	14
3700	3807	141 ± 5	143	25	15	11	7
3725	3826	156 ± 8	153	25	19	13	15
3750	3851	169 ± 8	166	25	25	18	13
3800	3915	202 ± 5	201	50	64	45	33
3850	3960	223 ± 9	227	50	45	32	21
3900	4006	248 ± 6	254	50	46	32	25
4000	4095	309 ± 9	309	100	89	63	61

"All values are in nanometers. ${}^bw_{\text{design}}$ is the designed base line width of the v-shaped polymer pens; w_{measured} is the measured line width of each PPCLL line pattern; $L_{\text{simulated}}$ is the simulated contact line width based on eq 3 L = f(w, z), for $w = w_{\text{measured}}$ and z = 547 nm; Δw_{design} , $\Delta w_{\text{measured}}$, and $\Delta L_{\text{measured}}$ are the increments corresponding to w_{design} , w_{measured} , and L_{measured} ; $\Delta h_{\text{calculated}}$ is the height increment of v-shaped polymer pen calculated from $\Delta h_{\text{calculated}} = \frac{1}{\sqrt{2}} \Delta w_{\text{measured}}$.

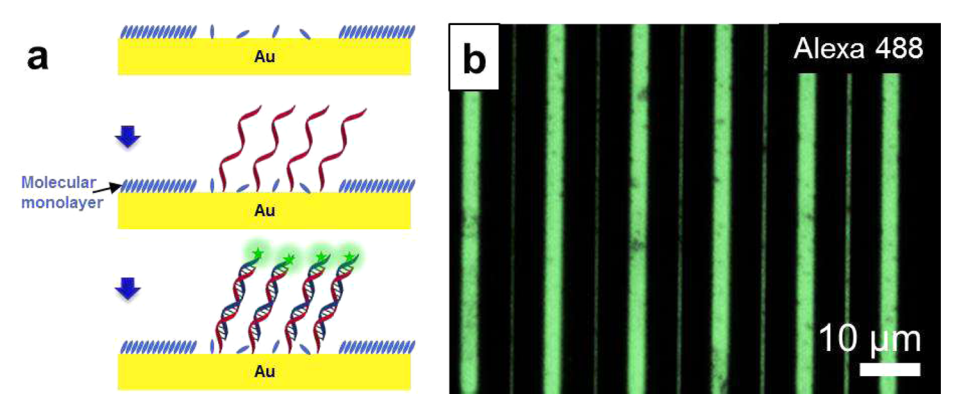


Figure 5. (a) After PPCLL patterning, thiolated DNA molecules are inserted into the patterned regions and fluorescently labeled complementary target DNA is hybridized on the substrate. (b) A typical fluorescence microscopy image after hybridization. (False color (green) is used to enhance the pattern.)

with line width increments of 25, 50, and 100 nm. For the 25 nm increment (shown in bold in Table 1), the corresponding height increment of the polymer pens was $\frac{25 \text{ nm}}{\sqrt{2}} = 18 \text{ nm}$. As shown in Figure 4a, the v-shaped polymer pens were separated by the support elements. Electron-beam lithography was used to produce base line widths with small increments (25–100 nm) for proof-of-concept purposes (details of EBL are in the Supporting Information). The differences between the designed base line widths (w_{design}) and the measured base line widths (w_{measured}) of the v-shaped polymer pens were 100 nm, as listed in Table 1.

Using this stamp design, a PPCLL experiment without an extra compression force beyond the weight of the stamp was performed. As seen in the SEM image in Figure 4, v-shaped polymer pens with larger base line widths generated larger PPCLL feature line widths, which indicated larger contact areas, as expected. A full set of SEM images are shown in Figure S4. As listed in Table 1, we obtained a series of line widths of 31 ± 4 , 48 ± 4 , 67 ± 4 , 81 ± 7 , 101 ± 7 , and 120 ± 5 , 134 ± 7 , 141 ± 5 , 156 ± 8 , 169 ± 8 , 202 ± 5 , 223 ± 9 , 248 ± 6 , and 309 ± 9 nm. Among these, the smallest line width was 31 ± 4 nm. For those line features with line widths <100 nm, on the SEM

images "dark" regions appear at the Au crystal grain boundaries, giving the images slightly undulating shapes. For the smallest feature sizes one can achieve in PPCLL, the original tip sizes of the polymer pens are the primary limiting factor, that is, feature size limit = tip size (sub-20 nm). For $w_{\rm design}$ from 3550 to 3750 nm, the designed base line width increment $\Delta w_{\rm design}$ was fixed at 25 nm resulting in an average measured base line width increment of $\Delta w_{\rm measured} = 26 \pm 6$ nm, and an average calculated height increment of $\Delta h_{\rm calculated} = 18 \pm 4$ nm based on $\Delta w_{\rm measured}$ increment (shown in bold in Table 1). Such small increments resulted in average measured pattern line width increments $\Delta L_{\rm measured}$ at the sub-20 nm scale, 15 \pm 4 nm. Both the sub-40 nm line width and the sub-20 nm line width increments are comparable to the critical dimensions and resolutions of many vacuum-based nanolithography techniques.

Next, we compared the measured results with the universal eq 2 from the simulation results. The measured feature line widths $L_{\rm measured}$ and the measured base line widths $w_{\rm measured}$ of the corresponding v-shaped polymer pens are plotted in Figure 4c. To calculate the corresponding vertical compression distance z in eq 2, we first applied the largest measured $w_{\rm measured} = 4095$ nm and $L_{\rm measured} = 309$ nm in eq 2 to get z = 547 nm. Then, by fixing z at 547 nm, we obtained eq 3 where

we found a'' = 1431 nm, b'' = -1.188, and $c'' = 2.232 \times 10^{-4}$ nm⁻¹. We plotted eq 3 in Figure 4c and found that the calculated data fit the experimental data well. On the basis of $w_{\rm measured}$, we calculated $L_{\rm simulated}$. The almost negligible differences (\sim 5 nm average) between the $L_{\rm measured}$ and $L_{\rm simulated}$ could be due to imperfect estimates of the PDMS properties used in the simulations.

So far, we have demonstrated PPCLL using PDMS stamps of 1.5 cm × 1.5 cm but larger areas are certainly possible. For directly patterning wafer-scale substrates, the primary challenges will be (1) how to achieve high-quality polymer pens over large areas, and (2) how to achieve conformal contact over large areas. For the first challenge, one can integrate a rigid support (e.g., glass) with the back of the stamp to produce uniform features across an entire 3 in. wafer surface. To the second challenge, one can integrate optical/force-feedback leveling systems to achieve uniform contact over large areas. Our support element system can also be used for the purpose of large-area leveling. With either solution or a combination of both, it is expected that high-quality wafer-scale patterning across large areas can be achieved.

To visualize the fabricated patterns, to test the applicability of PPCLL, and to demonstrate the potential for biological patterning applications, DNA hybridization experiments were performed. We have demonstrated that CLL can be used to produce DNA patterns with high hybridization efficiencies. Using PPCLL to pattern DNA in a similar fashion represents an economical and high-throughput avenue for fabricating functional DNA micro/nano arrays. 7,23,60,83 As shown in the scheme in Figure 5a, SAM molecules were removed from the contacted regions by PPCLL and thiolated single-stranded DNA molecules were inserted into the patterned regions through Au—S bonding.

Single-stranded patterned DNA was hybridized with fluorescently labeled complementary DNA enabling visualization of the chemical lift-off patterns via fluorescence microscopy. In Figure 5b, an image of a PPCLL pattern is shown illustrating regions (lines of varying widths) of patterned, hybridized DNA. The patterns are consistent with SEM data, which provides additional confirmation that PPCLL has indeed occurred. The DNA hybridization experiments show that PPCLL can be used to pattern biomolecules that retain functionality, that is, hybridization in this case. Being able to adjust pattern sizes and to create large-area substrates with binding sites and bioactive species illustrates that PPCLL might be used to fabricate biological devices, such as, biosensors, nucleotide arrays, and selective capture substrates. (Experimental details are provided in the Supporting Information.)

In summary, we demonstrated and tested PPCLL through simulation and experiments. Polymer-pen chemical lift-off lithography offers high pattern fidelity, low-cost, large-area, nanometer-scale resolution patterning capabilities by combining the advantages of polymer-pen lithography and chemical lift-off lithography. Through the use of stamp support elements and polymer pens with designed size gradients, we demonstrated sub-40 nm feature patterning and sub-20 nm feature line width increments without a piezoelectric scanning stage or a leveling system used in many conventional nanolithography techniques. Nonetheless, we plan to couple PPCLL with a piezoelectric scanning stage system to realize higher resolution patterning. Polymer-pen chemical lift-off lithography is a promising nanofabrication technique for a broad range of applications in electronics, optics, energy, and biology.

ASSOCIATED CONTENT

S Supporting Information

The Supporting Information is available free of charge on the ACS Publications website at DOI: 10.1021/acs.nanolett.7b01236.

Figures and experimental details describe fabrication of Si masters and PDMS stamps, characterization of morphology (chemical patterns, stamps) and surface roughness (masters, stamps), surface functionalization of substrate (Au/Cr/Si), activation of PDMS stamps, DNA patterning, and fluorescence microscopy (PDF)

AUTHOR INFORMATION

Corresponding Authors

*E-mail: aandrews@mednet.ucla.edu.

*E-mail: psw@cnsi.ucla.edu.

ORCID ®

Xiaobin Xu: 0000-0002-3479-0130 Qing Yang: 0000-0003-4422-5300 Chuanzhen Zhao: 0000-0003-0162-1231 Chad A. Mirkin: 0000-0002-6634-7627 Anne M. Andrews: 0000-0002-1961-4833 Paul S. Weiss: 0000-0001-5527-6248

Author Contributions

X.X. and Q.Y. contributed equally. The experiments were designed by X.X., Q.Y., and P.S.W. Data were collected by X.X., Q.Y., K.M.C., C.Z., N.W., and J.N.B. and were analyzed by X.X., Q.Y., P.S.W., and A.M.A. Figures were prepared by X.X. and Q.Y. The manuscript was written by X.X., Q.Y., P.S.W., and A.M.A. with assistance from all other authors.

Notes

The authors declare the following competing financial interest(s): Chad A. Mirkin is a scientific founder of TERA-Print.

■ ACKNOWLEDGMENTS

This work was supported by National Science Foundation Grant CMMI-1636136. C.Z. thanks the China Scholarship Council for a CSC-UCLA scholarship. N.W. thanks the Royal Thai Government for a graduate fellowship. L.S.S. thanks the Merkin Family Foundation for the Merkin Family Foundation Postdoctoral Fellowship. This material is based upon work supported by the Air Force Office of Scientific Research under Awards FA9550-12-1-0141 and FA9550-16-1-0150. The authors thank Dr. Andrew Guttentag, Dr. Huan Cao, Dr. Jeffrey Schwartz, Logan Stewart, and Thomas Young for discussions and their help. We also acknowledge the facilities and thank the staff of the Electron Imaging Center, Nano & Pico Characterization Lab, and Integrated Systems Nanofabrication Cleanroom of the California NanoSystems Institute, especially Krissy Do and Lorna Tokunaga.

REFERENCES

- (1) Jeon, H.-J.; Kim, K. H.; Baek, Y.-K.; Kim, D. W.; Jung, H.-T. New Top-Down Approach for Fabricating High-Aspect-Ratio Complex Nanostructures with 10 nm Scale Features. *Nano Lett.* **2010**, *10*, 3604—3610.
- (2) Pires, D.; Hedrick, J. L.; De Silva, A.; Frommer, J.; Gotsmann, B.; Wolf, H.; Despont, M.; Duerig, U.; Knoll, A. W. Nanoscale Three-Dimensional Patterning of Molecular Resists by Scanning Probes. *Science* **2010**, *328*, 732–735.

(3) Carlson, A.; Bowen, A. M.; Huang, Y.; Nuzzo, R. G.; Rogers, J. A. Transfer Printing Techniques for Materials Assembly and Micro/Nanodevice Fabrication. *Adv. Mater.* **2012**, *24*, 5284–5318.

- (4) Smith, J. T.; Franklin, A. D.; Farmer, D. B.; Dimitrakopoulos, C. D. Reducing Contact Resistance in Graphene Devices through Contact Area Patterning. *ACS Nano* **2013**, *7*, 3661–3667.
- (5) Priolo, F.; Gregorkiewicz, T.; Galli, M.; Krauss, T. F. Silicon Nanostructures for Photonics and Photovoltaics. *Nat. Nanotechnol.* **2014**, *9*, 19–32.
- (6) Tsai, H.; Pitera, J. W.; Miyazoe, H.; Bangsaruntip, S.; Engelmann, S. U.; Liu, C.-C.; Cheng, J. Y.; Bucchignano, J. J.; Klaus, D. P.; Joseph, E. A.; Sanders, D. P.; Colburn, M. E.; Guillorn, M. A. Two-Dimensional Pattern Formation Using Graphoepitaxy of PS-b-PMMA Block Copolymers for Advanced Finfet Device and Circuit Fabrication. ACS Nano 2014, 8, 5227–5232.
- (7) Kim, J.; Rim, Y. S.; Chen, H.; Cao, H. H.; Nakatsuka, N.; Hinton, H. L.; Zhao, C.; Andrews, A. M.; Yang, Y.; Weiss, P. S. Fabrication of High-Performance Ultrathin In₂O₃ Film Field-Effect Transistors and Biosensors Using Chemical Lift-Off Lithography. *ACS Nano* **2015**, *9*, 4572–4582.
- (8) Ozbay, E. Plasmonics: Merging Photonics and Electronics at Nanoscale Dimensions. *Science* **2006**, *311*, 189–193.
- (9) Henzie, J.; Lee, M. H.; Odom, T. W. Multiscale Patterning of Plasmonic Metamaterials. *Nat. Nanotechnol.* **2007**, *2*, 549–554.
- (10) Kung, S.-C.; Van Der Veer, W. E.; Yang, F.; Donavan, K. C.; Penner, R. M. 20 ms Photocurrent Response from Lithographically Patterned Nanocrystalline Cadmium Selenide Nanowires. *Nano Lett.* **2010**, *10*, 1481–1485.
- (11) Fan, F.-R.; Lin, L.; Zhu, G.; Wu, W.; Zhang, R.; Wang, Z. L. Transparent Triboelectric Nanogenerators and Self-Powered Pressure Sensors Based on Micropatterned Plastic Films. *Nano Lett.* **2012**, *12*, 3109–3114.
- (12) Ul-Haq, E.; Patole, S.; Moxey, M.; Amstad, E.; Vasilev, C.; Hunter, C. N.; Leggett, G. J.; Spencer, N. D.; Williams, N. H. Photocatalytic Nanolithography of Self-Assembled Monolayers and Proteins. *ACS Nano* **2013**, *7*, 7610–7618.
- (13) Moxey, M.; Johnson, A.; El-Zubir, O.; Cartron, M.; Dinachali, S. S.; Hunter, C. N.; Saifullah, M. S. M.; Chong, K. S. L.; Leggett, G. J. Fabrication of Self-Cleaning, Reusable Titania Templates for Nanometer and Micrometer Scale Protein Patterning. ACS Nano 2015, 9, 6262–6270.
- (14) Cao, Q.; Kim, H.-S.; Pimparkar, N.; Kulkarni, J. P.; Wang, C.; Shim, M.; Roy, K.; Alam, M. A.; Rogers, J. A. Medium-Scale Carbon Nanotube Thin-Film Integrated Circuits on Flexible Plastic Substrates. *Nature* **2008**, *454*, 495–500.
- (15) Hwang, J. K.; Cho, S.; Dang, J. M.; Kwak, E. B.; Song, K.; Moon, J.; Sung, M. M. Direct Nanoprinting by Liquid-Bridge-Mediated Nanotransfer Moulding. *Nat. Nanotechnol.* **2010**, *5*, 742–748.
- (16) Cheong, L. L.; Paul, P.; Holzner, F.; Despont, M.; Coady, D. J.; Hedrick, J. L.; Allen, R.; Knoll, A. W.; Duerig, U. Thermal Probe Maskless Lithography for 27.5 nm Half-Pitch Si Technology. *Nano Lett.* **2013**, *13*, 4485–4491.
- (17) Kim, T.-H.; Cho, K.-S.; Lee, E. K.; Lee, S. J.; Chae, J.; Kim, J. W.; Kim, D. H.; Kwon, J.-Y.; Amaratunga, G.; Lee, S. Y.; Choi, B. L.; Kuk, Y.; Kim, J. M.; Kim, K. Full-Colour Quantum Dot Displays Fabricated by Transfer Printing. *Nat. Photonics* **2011**, *5*, 176–182.
- (18) Jiang, M.; Kurvits, J. A.; Lu, Y.; Nurmikko, A. V.; Zia, R. Reusable Inorganic Templates for Electrostatic Self-Assembly of Individual Quantum Dots, Nanodiamonds, and Lanthanide-Doped Nanoparticles. *Nano Lett.* **2015**, *15*, 5010–5016.
- (19) Xie, W.; Gomes, R.; Aubert, T.; Bisschop, S.; Zhu, Y.; Hens, Z.; Brainis, E.; Van Thourhout, D. Nanoscale and Single-Dot Patterning of Colloidal Quantum Dots. *Nano Lett.* **2015**, *15*, 7481–7487.
- (20) Liang, X.; Morton, K. J.; Austin, R. H.; Chou, S. Y. Single Sub-20 nm Wide, Centimeter-Long Nanofluidic Channel Fabricated by Novel Nanoimprint Mold Fabrication and Direct Imprinting. *Nano Lett.* **2007**, *7*, 3774–3780.

(21) Stewart, M. E.; Anderton, C. R.; Thompson, L. B.; Maria, J.; Gray, S. K.; Rogers, J. A.; Nuzzo, R. G. Nanostructured Plasmonic Sensors. *Chem. Rev.* **2008**, *108*, 494–521.

- (22) Xu, X. B.; Kim, K.; Li, H. F.; Fan, D. L. Ordered Arrays of Raman Nanosensors for Ultrasensitive and Location Predictable Biochemical Detection. *Adv. Mater.* **2012**, *24*, 5457–5463.
- (23) Scheible, M. B.; Pardatscher, G.; Kuzyk, A.; Simmel, F. C. Single Molecule Characterization of DNA Binding and Strand Displacement Reactions on Lithographic DNA Origami Microarrays. *Nano Lett.* **2014**, *14*, 1627–1633.
- (24) Rim, Y. S.; Bae, S.-H.; Chen, H.; Yang, J. L.; Kim, J.; Andrews, A. M.; Weiss, P. S.; Yang, Y.; Tseng, H.-R. Printable Ultrathin Metal Oxide Semiconductor-Based Conformal Biosensors. *ACS Nano* **2015**, *9*, 12174–12181.
- (25) Xu, X. B.; Kim, K.; Fan, D. L. Tunable Release of Multiplex Biochemicals by Plasmonically Active Rotary Nanomotors. *Angew. Chem., Int. Ed.* **2015**, *54*, 2525–2529.
- (26) Kim, K.; Guo, J. H.; Xu, X. B.; Fan, D. L. Micromotors with Step-Motor Characteristics by Controlled Magnetic Interactions among Assembled Components. *ACS Nano* **2015**, *9*, 548–554.
- (27) Brown, P. O.; Botstein, D. Exploring the New World of the Genome with DNA Microarrays. *Nat. Genet.* **1999**, *21*, 33–37.
- (28) Pollack, J. R.; Perou, C. M.; Alizadeh, A. A.; Eisen, M. B.; Pergamenschikov, A.; Williams, C. F.; Jeffrey, S. S.; Botstein, D.; Brown, P. O. Genome-Wide Analysis of DNA Copy-Number Changes Using Cdna Microarrays. *Nat. Genet.* **1999**, 23, 41–46.
- (29) Lickwar, C. R.; Mueller, F.; Hanlon, S. E.; Mcnally, J. G.; Lieb, J. D. Genome-Wide Protein-DNA Binding Dynamics Suggest a Molecular Clutch for Transcription Factor Function. *Nature* **2012**, 484, 251–255.
- (30) Loven, J.; Orlando, D. A.; Sigova, A. A.; Lin, C. Y.; Rahl, P. B.; Burge, C. B.; Levens, D. L.; Lee, T. I.; Young, R. A. Revisiting Global Gene Expression Analysis. *Cell* **2012**, *151*, 476–482.
- (31) Cao, H. H.; Nakatsuka, N.; Serino, A. C.; Liao, W. S.; Cheunkar, S.; Yang, H.; Weiss, P. S.; Andrews, A. M. Controlled DNA Patterning by Chemical Lift-Off Lithography: Matrix Matters. *ACS Nano* **2015**, *9*, 11439–11454.
- (32) Ko, H. C.; Stoykovich, M. P.; Song, J.; Malyarchuk, V.; Choi, W. M.; Yu, C.-J.; Geddes Iii, J. B.; Xiao, J.; Wang, S.; Huang, Y.; Rogers, J. A. A Hemispherical Electronic Eye Camera Based on Compressible Silicon Optoelectronics. *Nature* **2008**, *454*, 748–753.
- (33) Rogers, J. A.; Someya, T.; Huang, Y. Materials and Mechanics for Stretchable Electronics. *Science* **2010**, 327, 1603–1607.
- (34) Windmiller, J. R.; Wang, J. Wearable Electrochemical Sensors and Biosensors: A Review. *Electroanalysis* **2013**, *25*, 29–46.
- (35) Pang, C.; Lee, C.; Suh, K.-Y. Recent Advances in Flexible Sensors for Wearable and Implantable Devices. *J. Appl. Polym. Sci.* **2013**, *130*, 1429–1441.
- (36) Kim, J.; Rim, Y. S.; Liu, Y.; Serino, A. C.; Thomas, J. C.; Chen, H.; Yang, Y.; Weiss, P. S. Interface Control in Organic Electronics Using Mixed Monolayers of Carboranethiol Isomers. *Nano Lett.* **2014**, 14, 2946–2951.
- (37) Switkes, M.; Rothschild, M. Immersion Lithography at 157 nm. J. Vac. Sci. Technol., B: Microelectron. Process. Phenom. 2001, 19, 2353.
- (38) Ghaida, R. S.; Agarwal, K. B.; Liebmann, L. W.; Nassif, S. R.; Gupta, P. A Novel Methodology for Triple/Multiple-Patterning Layout Decomposition. *Proc. SPIE* **2012**, 8327, 83270M.
- (39) Han, S. H.; Doherty, C. M.; Marmiroli, B.; Jo, H. J.; Buso, D.; Patelli, A.; Schiavuta, P.; Innocenzi, P.; Lee, Y. M.; Thornton, A. W.; Hill, A. J.; Falcaro, P. Simultaneous Microfabrication and Tuning of the Permselective Properties in Microporous Polymers Using X-Ray Lithography. *Small* **2013**, *9*, 2277–2282.
- (40) Miszta, K.; Greullet, F.; Marras, S.; Prato, M.; Toma, A.; Arciniegas, M.; Manna, L.; Krahne, R. Nanocrystal Film Patterning by Inhibiting Cation Exchange via Electron-Beam or X-Ray Lithography. *Nano Lett.* **2014**, *14*, 2116–2122.
- (41) Chang, S. W.; Ayothi, R.; Bratton, D.; Yang, D.; Felix, N.; Cao, H. B.; Deng, H.; Ober, C. K. Sub-50 nm Feature Sizes Using Positive

Tone Molecular Glass Resists for EUV Lithography. J. Mater. Chem. 2006, 16, 1470-1474.

- (42) Langner, A.; Paivanranta, B.; Terhalle, B.; Ekinci, Y. Fabrication of Quasiperiodic Nanostructures with EUV Interference Lithography. *Nanotechnology* **2012**, *23*, 105303.
- (43) Frommhold, A.; Mcclelland, A.; Yang, D. X.; Palmer, R. E.; Roth, J.; Ekinci, Y.; Rosamund, M. C.; Robinson, A. P. G. Towards 11 nm Half-Pitch Resolution for a Negative-Tone Chemically Amplified Molecular Resist Platform for EUV Lithography. *Proc. SPIE* **2015**, 9425, 942504.
- (44) Cumming, D. R. S.; Thoms, S.; Weaver, J. M. R.; Beaumont, S. P. 3 nm NiCr Wires Made Using Electron Beam Lithography and PMMA Resist. *Microelectron. Eng.* **1996**, *30*, 423–425.
- (45) Hu, W. C.; Sarveswaran, K.; Lieberman, M.; Bernstein, G. H. Sub-10 nm Electron Beam Lithography Using Cold Development of Poly(Methylmethacrylate). *J. Vac. Sci. Technol., B: Microelectron. Process. Phenom.* **2004**, *22*, 1711–1716.
- (46) Chen, S.; Svedendahl, M.; Antosiewicz, T. J.; Kall, M. Plasmon-Enhanced Enzyme-Linked Immunosorbent Assay on Large Arrays of Individual Particles Made by Electron Beam Lithography. *ACS Nano* **2013**, *7*, 8824–8832.
- (47) Kim, S.; Marelli, B.; Brenckle, M. A.; Mitropoulos, A. N.; Gil, E. S.; Tsioris, K.; Tao, H.; Kaplan, D. L.; Omenetto, F. G. All-Water-Based Electron-Beam Lithography Using Silk as a Resist. *Nat. Nanotechnol.* **2014**, *9*, 306–310.
- (48) Manfrinato, V. R.; Wen, J. G.; Zhang, L. H.; Yang, Y. J.; Hobbs, R. G.; Baker, B.; Su, D.; Zakharov, D.; Zaluzec, N. J.; Miller, D. J.; Stach, E. A.; Berggren, K. K. Determining the Resolution Limits of Electron-Beam Lithography: Direct Measurement of the Point-Spread Function. *Nano Lett.* **2014**, *14*, 4406–4412.
- (49) Bat, E.; Lee, J.; Lau, U. Y.; Maynard, H. D. Trehalose Glycopolymer Resists Allow Direct Writing of Protein Patterns by Electron-Beam Lithography. *Nat. Commun.* **2015**, *6*, 6654.
- (50) Gschrey, M.; Thoma, A.; Schnauber, P.; Seifried, M.; Schmidt, R.; Wohlfeil, B.; Kruger, L.; Schulze, J. H.; Heindel, T.; Burger, S.; Schmidt, F.; Strittmatter, A.; Rodt, S.; Reitzenstein, S. Highly Indistinguishable Photons from Deterministic Quantum-Dot Microlenses Utilizing Three-Dimensional in Situ Electron-Beam Lithography. *Nat. Commun.* **2015**, *6*, 7662.
- (51) Volkert, C. A.; Minor, A. M. Focused Ion Beam Microscopy and Micromachining. MRS Bull. **2007**, 32, 389–395.
- (52) Kalhor, N.; Boden, S. A.; Mizuta, H. Sub-10 nm Patterning by Focused He-Ion Beam Milling for Fabrication of Downscaled Graphene Nano Devices. *Microelectron. Eng.* **2014**, *114*, 70–77.
- (53) Pan, L.; Park, Y.; Xiong, Y.; Ulin-Avila, E.; Wang, Y.; Zeng, L.; Xiong, S.; Rho, J.; Sun, C.; Bogy, D. B.; Zhang, X. Maskless Plasmonic Lithography at 22 nm Resolution. *Sci. Rep.* **2011**, *1*, 175.
- (54) Kumar, A.; Whitesides, G. M. Features of Gold Having Micrometer to Centimeter Dimensions Can Be Formed through a Combination of Stamping with an Elastomeric Stamp and an Alkanethiol "Ink" Followed by Chemical Etching. *Appl. Phys. Lett.* 1993, 63, 2002.
- (55) Qin, D.; Xia, Y.; Whitesides, G. M. Soft Lithography for Microand Nanoscale Patterning. *Nat. Protoc.* **2010**, *5*, 491–502.
- (56) Xia, Y.; Whitesides, G. M. Soft Lithography. Angew. Chem., Int. Ed. 1998, 37, 550-575.
- (57) Xia, Y.; Zhao, X.-M.; Kim, E.; Whitesides, G. M. A Selective Etching Solution for Use with Patterned Self-Assembled Monolayers of Alkanethiolates on Gold. *Chem. Mater.* **1995**, *7*, 2332–2337.
- (58) Delamarche, E.; Schmid, H.; Bietsch, A.; Larsen, N. B.; Rothuizen, H.; Michel, B.; Biebuyck, H. Transport Mechanisms of Alkanethiols During Microcontact Printing on Gold. *J. Phys. Chem. B* **1998**, *102*, 3324–3334.
- (59) Srinivasan, C.; Mullen, T. J.; Hohman, J. N.; Anderson, M. E.; Dameron, A. A.; Andrews, A. M.; Dickey, E. C.; Horn, M. W.; Weiss, P. S. Scanning Electron Microscopy of Nanoscale Chemical Patterns. *ACS Nano* **2007**, *1*, 191–201.

- (60) Liao, W.-S.; Cheunkar, S.; Cao, H. H.; Bednar, H. R.; Weiss, P. S.; Andrews, A. M. Subtractive Patterning via Chemical Lift-Off Lithography. *Science* **2012**, 337, 1517–1521.
- (61) Xu, S.; Liu, G.-Y. Nanometer-Scale Fabrication by Simultaneous Nanoshaving and Molecular Self-Assembly. *Langmuir* **1997**, *13*, 127–129.
- (62) Xu, S.; Miller, S.; Laibinis, P. E.; Liu, G.-Y. Fabrication of Nanometer Scale Patterns within Self-Assembled Monolayers by Nanografting. *Langmuir* 1999, 15, 7244–7251.
- (63) Li, X.-M.; Péter, M.; Huskens, J.; Reinhoudt, D. N. Catalytic Microcontact Printing without Ink. *Nano Lett.* **2003**, *3*, 1449–1453.
- (64) Mclellan, J. M.; Geissler, M.; Xia, Y. Edge Spreading Lithography and Its Application to the Fabrication of Mesoscopic Gold and Silver Rings. J. Am. Chem. Soc. 2004, 126, 10830–10831.
- (65) Sullivan, T. P.; Van Poll, M. L.; Dankers, P. Y. W.; Huck, W. T. S. Forced Peptide Synthesis in Nanoscale Confinement under Elastomeric Stamps. *Angew. Chem., Int. Ed.* **2004**, 43, 4190–4193.
- (66) Wendeln, C.; Ravoo, B. J. Surface Patterning by Microcontact Chemistry. *Langmuir* **2012**, 28, 5527–5538.
- (67) Dameron, A. A.; Hampton, J. R.; Smith, R. K.; Mullen, T. J.; Gillmor, S. D.; Weiss, P. S. Microdisplacement Printing. *Nano Lett.* **2005**, *5*, 1834–1837.
- (68) Saavedra, H. M.; Mullen, T. J.; Zhang, P. P.; Dewey, D. C.; Claridge, S. A.; Weiss, P. S. Hybrid Strategies in Nanolithography. *Rep. Prog. Phys.* **2010**, *73*, 036501.
- (69) Shuster, M. J.; Vaish, A.; Cao, H. H.; Guttentag, A. I.; Mcmanigle, J. E.; Gibb, A. L.; Martinez, M. M.; Nezarati, R. M.; Hinds, J. M.; Liao, W. S.; Weiss, P. S.; Andrews, A. M. Patterning Small-Molecule Biocapture Surfaces: Microcontact Insertion Printing Vs. Photolithography. *Chem. Commun.* **2011**, *47*, 10641–10643.
- (70) Claridge, S. A.; Liao, W. S.; Thomas, J. C.; Zhao, Y.; Cao, H. H.; Cheunkar, S.; Serino, A. C.; Andrews, A. M.; Weiss, P. S. From the Bottom Up: Dimensional Control and Characterization in Molecular Monolayers. *Chem. Soc. Rev.* **2013**, *42*, 2725–2745.
- (71) Andrews, A. M.; Liao, W.-S.; Weiss, P. S. Double-Sided Opportunities Using Chemical Lift-Off Lithography. *Acc. Chem. Res.* **2016**, *49*, 1449–1457.
- (72) Piner, R. D.; Zhu, J.; Xu, F.; Hong, S.; Mirkin, C. A. "Dip-Pen" Nanolithography. *Science* **1999**, 283, 661–663.
- (73) Huo, F.; Zheng, Z.; Zheng, G.; Giam, L. R.; Zhang, H.; Mirkin, C. A. Polymer Pen Lithography. *Science* **2008**, *321*, 1658–1660.
- (74) Zheng, Z.; Daniel, W. L.; Giam, L. R.; Huo, F.; Senesi, A. J.; Zheng, G.; Mirkin, C. A. Multiplexed Protein Arrays Enabled by Polymer Pen Lithography: Addressing the Inking Challenge. *Angew. Chem., Int. Ed.* **2009**, *48*, 7626–7629.
- (75) Liao, X.; Braunschweig, A. B.; Mirkin, C. A. "Force-Feedback" Leveling of Massively Parallel Arrays in Polymer Pen Lithography. *Nano Lett.* **2010**, *10*, 1335–1340.
- (76) Liao, X.; Braunschweig, A. B.; Zheng, Z.; Mirkin, C. A. Forceand Time-Dependent Feature Size and Shape Control in Molecular Printing via Polymer-Pen Lithography. *Small* **2010**, *6*, 1082–1086.
- (77) Eichelsdoerfer, D. J.; Liao, X.; Cabezas, M. D.; Morris, W.; Radha, B.; Brown, K. A.; Giam, L. R.; Braunschweig, A. B.; Mirkin, C. A. Large-Area Molecular Patterning with Polymer Pen Lithography. *Nat. Protoc.* **2013**, *8*, 2548–2560.
- (78) Liao, X.; Huang, Y.-K.; Mirkin, C. A.; Dravid, V. P. High Throughput Synthesis of Multifunctional Oxide Nanostructures within Nanoreactors Defined by Beam Pen Lithography. *ACS Nano* **2017**, DOI: 10.1021/acsnano.7b00124.
- (79) Demers, L. M.; Ginger, D. S.; Park, S. J.; Li, Z.; Chung, S. W.; Mirkin, C. A. Direct Patterning of Modified Oligonucleotides on Metals and Insulators by Dip-Pen Nanolithography. *Science* **2002**, *296*, 1836–1838.
- (80) Odom, T. W.; Love, J. C.; Wolfe, D. B.; Paul, K. E.; Whitesides, G. M. Improved Pattern Transfer in Soft Lithography Using Composite Stamps. *Langmuir* **2002**, *18*, 5314–5320.
- (81) Vaish, A.; Shuster, M. J.; Cheunkar, S.; Weiss, P. S.; Andrews, A. M. Tuning Stamp Surface Energy for Soft Lithography of Polar

Molecules to Fabricate Bioactive Small-Molecule Microarrays. *Small* **2011**, *7*, 1471–1479.

- (82) Xie, Z.; Shen, Y.; Zhou, X.; Yang, Y.; Tang, Q.; Miao, Q.; Su, J.; Wu, H.; Zheng, Z. Polymer Pen Lithography Using Dual-Elastomer Tip Arrays. *Small* **2012**, *8*, 2664–2669.
- (83) Noh, H.; Hung, A. M.; Choi, C.; Lee, J. H.; Kim, J.-Y.; Jin, S.; Cha, J. N. 50 nm DNA Nanoarrays Generated from Uniform Oligonucleotide Films. *ACS Nano* **2009**, *3*, 2376–2382.